2007 IEEE International Conference on
Robotics and Automation
Roma, Italy, 10-14 April 2007

On Control for "Blind Touching" by Human-Like Thumb Robots

Kenji Tahara, Suguru Arimoto, Zhi-Wei Luo and Morio Yoshida

Abstract— **Human can pinch or grasp and manipulate an object stably and dexterously. Accomplishment of such tasks is contributed from human hand's configuration, called "Fingers-thumb opposability". This opposability of the thumb against other digits is specific and granted to only human among primates. When we use a cell phone, or change a TV's channel using a remote controller, we grasp it by a palm and digits other than the thumb, and push buttons using the thumb quickly, without looking the buttons. These kinds of thumb's movement seem to be one of the most intelligent movements in a human. Therefore, execution of such touching tasks without visual or tactile sensing is called in this paper "Blind Touching". The goal of this research is to realize human-like "Blind Touching" by means of a 5 D.O.F. thumb robot model with soft and hemispherical finger-tip. To do this, we formulate a simultaneous contact position and touching force control by using 3-Dimensional rolling contact with the task plane. First, dynamics of the 5 D.O.F. thumb robot model with hemispherical soft finger-tip under rolling constraints is derived. Then, a sensory-motor control law without vision, force or tactile sensing is proposed. Some numerical simulations show that the desired contact position and touching force can be attained by the proposed control scheme. A theoretical proof of convergence to the desired state is also presented.**

I. INTRODUCTION

Dexterous movements of a human hand have attracted much attention of many robotics researchers to develop it in terms of both a structure and a control strategy. In anthropology, it is said that these dexterous movements are indebted to special configuration of human's thumb, called "Fingers-thumb opposition" [1]. This opposability of the thumb is one of the unique configurations which can only be seen in a human hand. When we use a cell phone, or change a TV's channel using a remote controller, we grasp it by a palm and digits other than the thumb, and push buttons using the thumb, without seeing themselves. These kinds of movements can be realized by using proprioceptive information which could have been obtained in the central nervous system. Now, we call such movements "Blind Touching".

As remarked above, the thumb plays a crucial role in our everyday life. In this paper, we treat a human-like 5 D.O.F. thumb robot model with a soft hemispherical finger-tip and show a coordinated sensory-motor control signal that realizes "Blind Touching". It controls simultaneously a contact position and touching force from the finger-tip to a task plane by using 3-Dimensional rolling movement.

During the past three decades a number of robot hands with single or plural fingers imitating mechanisms of human fingers were designed and many of them were actually made as reported in the literature [2–7]. However, there is a dearth of papers that were concerned with human-like functions of the thumb or index finger and, in particular, there is little research works that attempted to design control signals that can accomplish dynamically its desired functions. Very recently, however, Arimoto *et al.* [8–10] found an interesting class of sensory-motor coordination control schemes for realizing precision prehension (pinching) of a rigid object in a dynamic way by using a pair of robot fingers with multiple joints. They showed that if the hand is preshaped to grasp and placed in the vicinity of the object then the sensory-motor signal realizes stable pinching without knowing object kinematics and without using external sensings (tactile, force, or vision). This control scheme was called "Blind Grasping" and is now extended to applying for 3-Dimensional object grasping and manipulation [11]. The most noteworthy clue to the success is to have observed decisive roles of rolling constraints between finger-ends and object surfaces, from which tangential forces to the object surfaces arise. These tangential constraint forces can be used for control of forces and torques exerted to the object.

This paper also clarifies such important roles of rolling constraint in a different situation that the finger-end is soft and deformable and thereby an area contact arises. Therefore, rolling contacts are expressed as a movement of the center of contact circular area, which also induces a tangential force to the object surface that is fixed in the task plane. We will first derive Lagrange's equation of motion of the 5 D.O.F. robot thumb whose spherical soft end has such an area contact with the task plane. Then, we will propose a sensory-motor coordinated control signal based on the thumb's opposability and show that it realizes a desired hybrid position and force control in a "Blind Touching" manner.

II. A 5 D.O.F. THUMB ROBOT MODEL WITH HEMISPHERICAL SOFT FINGER-TIP

This section derives a 5 D.O.F. thumb robot model with a hemispherical soft finger-tip. It is known in physiology that the base joint of human thumb is a saddle joint. Human can move the contact point between the thumb and task plane by using 3-Dimensional rolling contact. In this paper, this saddle joint is expressed by the two rotational axes, Z-axis and Y-axis, whose crossing point is set as the origin of the fixed

This work was partially supported by the Ministry of Education, Science, Sports and Culture, Grant-in-Aid for Young Scientists (B), 18760205, 2006.

K. Tahara, S. Arimoto, Z.W. Luo and M. Yoshida are with the Bio-Mimetic Control Research Center, RIKEN, Nagoya, Aichi, 463-0003 JAPAN. {tahara, yoshida}@bmc.riken.jp

S. Arimoto is with the Department of Robotics, Ritsumeikan University, Kusatsu, Shiga, 525-8577 JAPAN. arimoto@se.ritsumei.ac.jp

Z.W. Luo is with the Department of Computer and Systems Engineering, Kobe University, Kobe, Hyogo, 657-8501 JAPAN. luo@gold.kobe-u.ac.jp

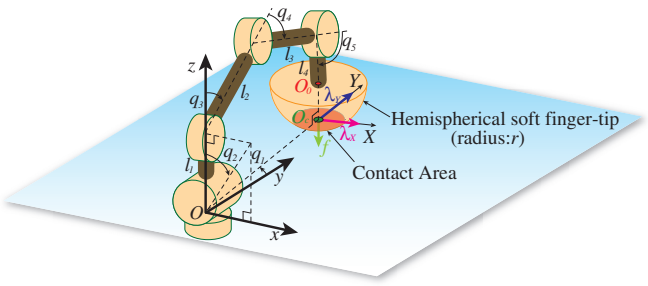

Fig. 1. A 5 D.O.F. thumb robot with a soft hemishperic tip model

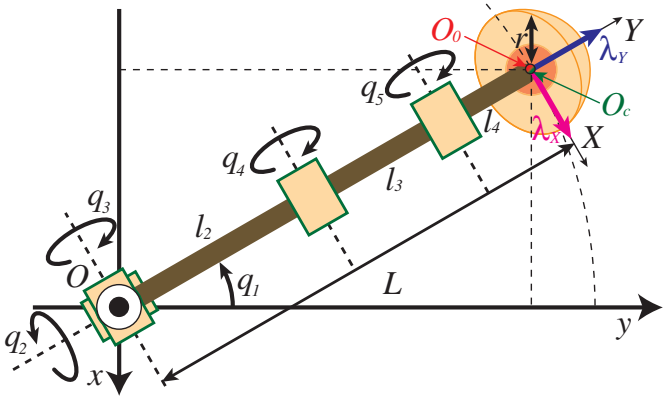

Fig. 2. A 5 D.O.F. thumb model on xy-plane

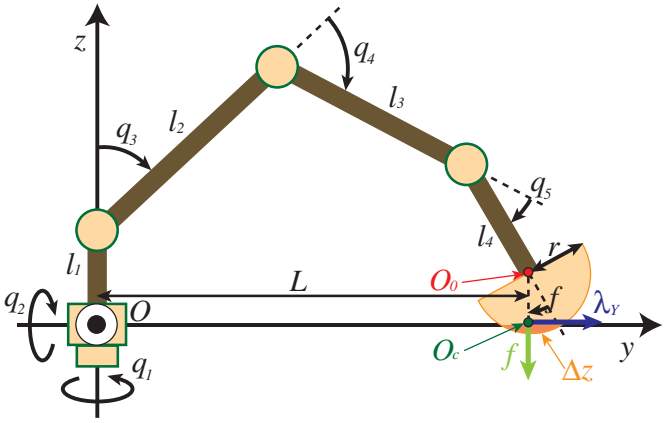

Fig. 3. A 5 D.O.F. thumb model on yz-plane

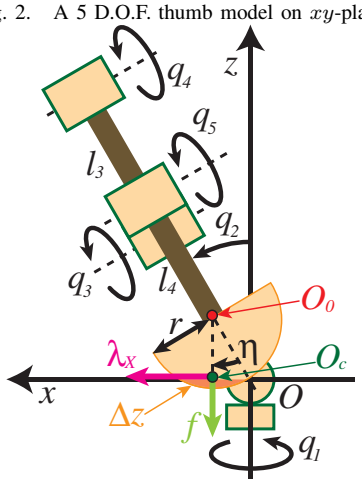

Fig. 4. A 5 D.O.F. thumb model on zx-plane

inertial frame. The 5 D.O.F. thumb robot model presented here is illustrated in Fig. 1. Assume that only rolling contacts between the finger-tip and task plane is allowed, and any frictions except the viscous friction arising due to finger-tip deformation are ignored. In this model, symbol O denotes the first and second joint center (center of the saddle joint) of the thumb and also the origin of Cartesian coordinates, O_0 denotes the center of hemispherical soft finger-tip whose position in Cartesian coordinates is expressed as $\boldsymbol{x_0} = (x_0, y_0, z_0)$, and O_c denotes the center of contact area whose Cartesian coordinates is expressed as $\boldsymbol{x_c} = (x_c, y_c, 0)$, and the radius of hemispherical finger-tip is r. Other symbols, $q_i (i{=}1{\sim}5)$, $l_j (j{=}1{\sim}4)$ are defined in Fig. 1. Figs. 2$\sim$4 show the thumb model on xy, yz and zx-plane, respectively. Also Fig. 5 shows spherical polar coordinates on the finger-tip to illustrate the 3-Dimensional rolling contact.

A. 3-Dimensional Rolling Constraints

Now, let us consider 3-Dimensional rolling constraints between the finger-tip and task plane. At the beginning, we introduce spherical polar coordinates at the center of the finger-tip O_c as shown in Figs 2$\sim$5. The spherical polar coordinates on the finger-tip can be expressed by joint angle

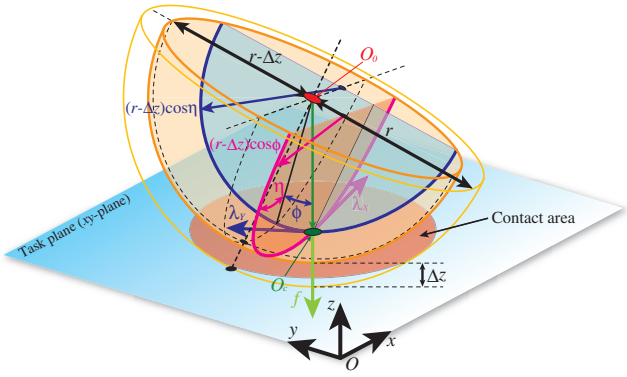

Fig. 5. Spherical polar coordinates at the center of the finger-tip

$\boldsymbol{q} = (q_1, q_2, q_3, q_4, q_5)^{\mathrm{T}} \in \mathbb{R}^5$ as follows:

$$\phi = \pi - q_3 - q_4 - q_5 \quad (1)$$

$$\eta = q_2 \quad (2)$$

And the maximum displacement Δz of deformation which arises in the center of contact area can be given as follows:

$$\Delta z = r - \cos q_2 \{l_1 + l_2 \cos q_3 + l_3 \cos(q_3 + q_4) + l_4 \cos(q_3 + q_4 + q_5)\} \quad (3)$$

Rotational movement of the finger-tip around the Z-axis at O_c called "Spinning" in this model cannot occur because the origin of Cartesian coordinates O and the center of area contact O_c are on the same task plane and these are constrained by the finger links. It is known that rolling-constraints are given by the condition that the velocity of the center of contact area on the spherical finger-tip relative to that on the task plane is zero during movements. Montana [12] formulated the 3-Dimensional rolling constraints in the case of which the rigid and free sphere object is in contact with the task plane from the kinematic viewpoint. Unlike the above case, in this paper, we consider the case that the soft and deformable hemispherical finger tip, which is not free and constrained to Cartesian coordinates by the finger links, makes not rigid pointwise but soft area contact with the task plane. In order to formulate these 3-Dimensional rolling constraints with area contact from the dynamical viewpoint, it should be noted that the rolling velocity vector on the surface of hemispherical finger-tip should be on the tangential plane (now, it is the task plane) at the center of contact area. By taking into account this necessary condition, two non-holonomic rolling constraints between the finger-tip and the task plane are given as follows:

$$(r-\Delta z)\frac{\mathrm{d}}{\mathrm{d}t}\left\{\cos\phi\cdot\eta\right\} = -\frac{\mathrm{d}}{\mathrm{d}t}\left(Lq_1\right) \tag{4}$$

$$(r-\Delta z)\frac{\mathrm{d}}{\mathrm{d}t}\left\{\cos\eta\cdot\phi\right\} = -\frac{\mathrm{d}}{\mathrm{d}t}L \tag{5}$$

where $L=\sqrt{x_c^2+y_c^2}$ stands for the distance between the center of contact area O_c and the origin of Cartesian coordinates O. Eq. (4) represents the rolling constraint toward X-axis at O_c (see Figs. 2 and 4). Similarly, eq. (5) represents the rolling constraint toward Y-axis at O_c (see Figs. 2 and 3). Eqs. (4) and (5) can be reformulated as Pfaffian constraints in the following [3]:

$$\boldsymbol{A}\dot{\boldsymbol{q}}=0 \tag{6}$$

where $\dot{\boldsymbol{q}}\in\mathbb{R}^5$ is the angular velocity vector and $\boldsymbol{A}\in\mathbb{R}^{2\times5}$ is the constraint matrix as follows:

$$\boldsymbol{A}=\begin{pmatrix}(r-\Delta z)\left(\cos\phi\dfrac{\partial\eta}{\partial\boldsymbol{q}}+\eta\dfrac{\partial(\cos\phi)}{\partial\boldsymbol{q}}\right)^{\mathrm{T}}+\left(q_1\dfrac{\partial L}{\partial\boldsymbol{q}}+L\dfrac{\partial q_1}{\partial\boldsymbol{q}}\right)^{\mathrm{T}}\\ (r-\Delta z)\left(\cos\eta\dfrac{\partial\phi}{\partial\boldsymbol{q}}+\phi\dfrac{\partial(\cos\eta)}{\partial\boldsymbol{q}}\right)^{\mathrm{T}}+\left(\dfrac{\partial L}{\partial\boldsymbol{q}}\right)^{\mathrm{T}}\end{pmatrix} \tag{7}$$

B. Dynamic Model of Soft Finger-Tip

We now discuss lumped-parametrization of the contact force caused by deformation of the finger-tip material which was introduced by Arimoto *et al.* [8]. The reproducing force $f(\Delta z)$ arizing in the normal direction to the task plane at the center of contact area O_c is given as follows:

$$\bar{f}(\Delta z)=k\Delta z^2 \tag{8}$$

where $k>0$ is a stiffness parameter depending upon the finger-tip material. In parallel to this, it is important to introduce a lamped-parametrized viscous force in such a form as

$$f(\Delta z,\Delta\dot{z})=\bar{f}(\Delta z)+\xi(\Delta z)\Delta\dot{z} \tag{9}$$

where $\xi(\Delta z)$ is a positive scalar function depending upon Δz.

C. Dynamics of The Thumb Robot

Let us derive the dynamics of this proposed thumb model. Total potential energy P and total kinetic energy K of the thumb model can be given as follows:

$$P = P_T(\boldsymbol{q})+P_F(\Delta z) \tag{10}$$

$$K = \frac{1}{2}\dot{\boldsymbol{q}}^{\mathrm{T}}\boldsymbol{H}(\boldsymbol{q})\dot{\boldsymbol{q}} \tag{11}$$

where $P_T(\boldsymbol{q})$ is the potential energy with respect to the gravitational effect for the thumb, and $P_F(\Delta z)$ is the elastic potential energy generated by deformation of the finger-tip as expressed by

$$P_F(\Delta z)=\int_0^{\Delta z}\bar{f}(\zeta)\mathrm{d}\zeta \tag{12}$$

$\boldsymbol{H}(\boldsymbol{q})\in\mathbb{R}^{5\times5}$ is the inertia matrix of the thumb. Therefore, Lagrange's equation of motion can be derived by applying Hamilton's variational principle. It is given as

$$\int_{t_0}^{t_1}\left[\delta\left(K-P\right)+\boldsymbol{A}^{\mathrm{T}}\boldsymbol{\lambda}-\frac{1}{2}\frac{\partial\xi(\Delta z)\Delta\dot{z}^2}{\partial\Delta\dot{z}}\delta\Delta z+\boldsymbol{u}^{\mathrm{T}}\delta\boldsymbol{q}\right]\mathrm{d}t=0 \tag{13}$$

where $\boldsymbol{\lambda}=\left(\lambda_X,\lambda_Y\right)^{\mathrm{T}}\in\mathbb{R}^2$ is the vector of Lagrange multipliers and its physical menaning is the rolling constraint force, and $\boldsymbol{u}\in\mathbb{R}^5$ is an input torque vector. Hence, Lagrange's equation is given as follows:

$$\boldsymbol{H}(\boldsymbol{q})\ddot{\boldsymbol{q}}+\left\{\frac{1}{2}\dot{\boldsymbol{H}}(\boldsymbol{q})+\boldsymbol{S}(\boldsymbol{q},\dot{\boldsymbol{q}})\right\}\dot{\boldsymbol{q}} -\boldsymbol{A}^{\mathrm{T}}\boldsymbol{\lambda}-f\frac{\partial\Delta x}{\partial\boldsymbol{q}}+\boldsymbol{g}(\boldsymbol{q})=\boldsymbol{u} \tag{14}$$

where $\boldsymbol{S}(\boldsymbol{q},\dot{\boldsymbol{q}})\in\mathbb{R}^{5\times5}$ is a skew-symmetric matrix and $\boldsymbol{g}(\boldsymbol{q})\in\mathbb{R}^5$ is the gravitational term coming from the potential energy $P_T(\boldsymbol{q})$ for the thumb. Now, taking inner product of the input $\boldsymbol{u}$ with the output $\dot{\boldsymbol{q}}$, and integrating it within time $t\in[0,T)$ yields

$$\int_0^t\dot{\boldsymbol{q}}^{\mathrm{T}}\boldsymbol{u}\,\mathrm{d}\tau=E(t)-E(0) +\int_0^t\xi(\Delta z(\tau))\Delta\dot{z}(\tau)^2\mathrm{d}\tau\le-E(0) \tag{15}$$

where $E=K+P$. This inequality means that the input-output pair satisfies passivity [13].

III. SENSORY-MOTOR CONTROL LAW TO REALIZE "BLIND TOUCHING"

We are now in a position to design a sensory-motor control signal that may realize "Blind Touching". Assume that the observable state variables are the joint angles $\boldsymbol{q}$ and angular velocities $\dot{\boldsymbol{q}}$. Also the radius r of hemispherical finger-tip is given, and a desired contact point position on the task plane $\boldsymbol{x_d} = (x_d, y_d, -\Delta z)$ is given from the proprioceptive information in advance. In the case of the robot thumb, Δz can be easily calculated from eq. (3) in real-time. Here, it is remarkable that the desired position of z-component is given as $z_d = -\Delta z$ which is not a constant, but a computable time-dependent variable. This variable finally converges to Δz_d and thereby the desired touching force f_d is established, where Δz_d is the maximum displacement of the finger-tip such that $\bar{f}(\Delta z_d) = f_d$. The input signal to control the contact point position and touching force is now defined as follows:

$$\boldsymbol{u} = \frac{f_d}{r}\boldsymbol{J_0}(\boldsymbol{q})^{\mathrm{T}}(\boldsymbol{x_0} - \boldsymbol{x_d}) - \boldsymbol{C}\dot{\boldsymbol{q}} + \boldsymbol{g}(\boldsymbol{q}) \tag{16}$$

where $\boldsymbol{J_0}(\boldsymbol{q}) \in \mathbb{R}^{5\times 3}$ is the Jacobian matrix concerning the center of hemispherical soft finger-tip $\boldsymbol{x_0}$ with respect to $\boldsymbol{q}$, $\boldsymbol{C} \in \mathbb{R}^{5\times 5}(> 0)$ is a damping matrix, and $\boldsymbol{g}(\boldsymbol{q})$ is to compensate the gravitational effect for the thumb. Also f_d/r stands for the gain to realize a desired touching force f_d and then, this controller proposed here is similar to the conventional task-space controller proposed by Takegaki and Arimoto [14]. It is remarkable in eq. (16) that this control signal can be constructed only by physical parameters of the thumb and measured information of its joint angles and angular velocities. Now, substituting eq. (16) into eq. (14) yields:

$$\boldsymbol{H}(\boldsymbol{q})\ddot{\boldsymbol{q}} + \left\{\frac{1}{2}\dot{\boldsymbol{H}}(\boldsymbol{q}) + \boldsymbol{S}(\boldsymbol{q},\dot{\boldsymbol{q}})\right\}\dot{\boldsymbol{q}} - \boldsymbol{A}^{\mathrm{T}}\boldsymbol{\lambda} - f\frac{\partial \Delta z}{\partial \boldsymbol{q}} - \frac{f_d}{r}\boldsymbol{J_0}(\boldsymbol{q})^{\mathrm{T}}(\boldsymbol{x_0} - \boldsymbol{x_d}) + \boldsymbol{C}\dot{\boldsymbol{q}} = \Delta\boldsymbol{u} = 0 \tag{17}$$

Then, taking inner product of the input $\Delta\boldsymbol{u}$ with the output $\dot{\boldsymbol{q}}$ yields:

$$\frac{\mathrm{d}}{\mathrm{d}t}V = -\dot{\boldsymbol{q}}^{\mathrm{T}}\boldsymbol{C}\dot{\boldsymbol{q}} - \xi(\Delta z(\tau))\Delta\dot{z}(\tau)^2 \le 0 \tag{18}$$

where V is a scalar function expressed by

$$V = K + P_F(\Delta z) + \frac{f_d}{2r}\left\{(x_0 - x_d)^2 + (y_0 - y_d)^2\right\} \ge 0 \tag{19}$$

In this formulation, the following relations are used.

$$\dot{\boldsymbol{q}}^{\mathrm{T}}\boldsymbol{A}^{\mathrm{T}} = 0 \tag{20}$$

$$\frac{\partial \Delta z^{\mathrm{T}}}{\partial \boldsymbol{q}} = -\boldsymbol{J_0}(\boldsymbol{q})^{\mathrm{T}}\boldsymbol{r_z}, \quad (\boldsymbol{r_z} = (0,0,1)^{\mathrm{T}}) \tag{21}$$

$$\Delta\dot{z}(\bar{f} - f_d) = \frac{\mathrm{d}}{\mathrm{d}t}\int_0^{\Delta z - \Delta z_d}\left\{\bar{f}(\zeta + \Delta z_d) - f_d\right\}\mathrm{d}\zeta = \frac{\mathrm{d}}{\mathrm{d}t}P_F(\Delta z) \tag{22}$$

Eq. (18) means that the closed-loop dynamics satisfies passivety. Since the scalar function $V(t)$ is positive definite on the constraint manifold and satisfies eq. (18), it follows that

$$\int_0^\infty \|\dot{\boldsymbol{q}}^{\mathrm{T}}(t)\boldsymbol{C}\dot{\boldsymbol{q}}(t)\|\mathrm{d}t < V(0) \tag{23}$$

Also $V(t)$ is non-increasing with increase of t as follows:

$$0 \le V(t) \le V(0) \tag{24}$$

Then $|x_0 - x_d|$ and $|y_0 - y_d|$ must be upper-bounded by some positive values εx and εy. Also the function $P_F(\delta z)$ with respect to $\delta z = \Delta z - \Delta z_d$ is positive definite in a neighborhood of $\delta z = 0$. Then δz must be upper-bounded by some value $\varepsilon z_M (= \Delta z_M - \Delta z_d)$ so that $P_F(\delta z_M) \le V(0)$. Hence $\xi(\Delta z(\tau))$ is upper-bounded and thereby it follows from eq. (18) that

$$\int_0^\infty |\Delta\dot{z}(t)|^2\mathrm{d}t < +\infty \tag{25}$$

Now, we assume for the time being for the sake of convenience that the joint angles $q_i(t)$ $(i = 1 \sim 5)$ are bounded during movements, i.e.,

$$|q_i(t) - q_i(0)| < \varepsilon q_i, \quad (i = 1 \sim 5) \tag{26}$$

where εq_i $(i = 1 \sim 5)$ are some positive values. Then the constraint matrix $\boldsymbol{A}$ is of rank($\boldsymbol{A}$) = 2 during movements, and we can obtain the constraint force vector $\boldsymbol{\lambda}$ analitically as follows:

$$\boldsymbol{\lambda} = \left(\boldsymbol{A}\boldsymbol{H}^{-1}\boldsymbol{A}^{\mathrm{T}}\right)^{-1}\left\{\boldsymbol{A}\boldsymbol{H}^{-1}\left(\frac{1}{2}\dot{\boldsymbol{H}} + \boldsymbol{S} + \boldsymbol{C}\right)\dot{\boldsymbol{q}} - \dot{\boldsymbol{A}}\dot{\boldsymbol{q}} - \boldsymbol{A}\boldsymbol{H}^{-1}\boldsymbol{B}\right\} \tag{27}$$

where

$$\boldsymbol{B} = \begin{pmatrix} \frac{f_d}{r}\frac{\partial x}{\partial \boldsymbol{q}} & \frac{f_d}{r}\frac{\partial y}{\partial \boldsymbol{q}} & \frac{\partial \Delta z}{\partial \boldsymbol{q}} \end{pmatrix}\begin{pmatrix} x_0 - x_d \\ y_0 - y_d \\ \bar{f} - f_d \end{pmatrix} \in \mathbb{R}^5 \tag{28}$$

and in this formulation, the derivertive of eq. (6)

$$\boldsymbol{A}\ddot{\boldsymbol{q}} = -\dot{\boldsymbol{A}}\dot{\boldsymbol{q}} \tag{29}$$

is used. Hence, the norm of the constraint force vector $\|\boldsymbol{\lambda}\|$ is upper-bounded as follows:

$$\|\boldsymbol{\lambda}\| \le \varepsilon\lambda \tag{30}$$

where $\varepsilon\lambda$ is some positive value. Then the norm of the vector of angular acceleration $\|\ddot{\boldsymbol{q}}\|$ should be upper-bounded as follows:

$$\|\ddot{\boldsymbol{q}}\| \le \varepsilon\ddot{q} \tag{31}$$

where $\varepsilon\ddot{q}$ is some positive value. Thus, $\dot{\boldsymbol{q}}(t) \in L^2(0,\infty)$ and $\Delta\dot{z}(t) \in L^2(0,\infty)$ should be uniformly continuous. From this result together with eqs. (23)$\sim$(25), we can conclude that

$$\dot{\boldsymbol{q}}(t) \to 0 \quad \text{and} \quad \Delta\dot{z}(t) \to 0 \quad \text{as} \quad t \to \infty \tag{32}$$

which implies that

$$-\boldsymbol{A}^{\mathrm{T}}\boldsymbol{\lambda} - \bar{f}\frac{\partial \Delta z}{\partial \boldsymbol{q}} - \frac{f_d}{r}\boldsymbol{J_0}(\boldsymbol{q})(\boldsymbol{x}_0 - \boldsymbol{x}_d) \to 0 \quad \text{as} \quad t \to \infty \tag{33}$$

Since $z_0 = r - \Delta z$ when the finger end is in contact with the xy-plane, it follows that

$$\begin{aligned}(\boldsymbol{x}_0 - \boldsymbol{x}_d)^{\mathrm{T}} &= (x_0 - x_d,\ y_0 - y_d,\ z_0 + \Delta z) \\ &= (x_0 - x_d,\ y_0 - y_d,\ r)\end{aligned} \tag{34}$$

By taking into account eq. (21), eq. (33) can be rewritten as follows:

$$-\boldsymbol{A}^{\mathrm{T}}\boldsymbol{\lambda} - \boldsymbol{B} \to 0 \quad \text{as} \quad t \to \infty \tag{35}$$

Since each column of the following matrix

$$\boldsymbol{W} = \left(\frac{\partial \Delta z}{\partial \boldsymbol{q}} \quad \frac{\partial x_0}{\partial \boldsymbol{q}} \quad \frac{\partial y_0}{\partial \boldsymbol{q}} \quad \boldsymbol{A}^{\mathrm{T}}\right) \in \mathbb{R}^{5\times 5} \tag{36}$$

are independent during movements, eq. (35) implies

$$\begin{cases} x_0(t) \to x_d,\ y_0(t) \to y_d, \\ \bar{f}(t) \to f_d,\ \boldsymbol{\lambda}(t) \to 0 \end{cases} \quad \text{as} \quad t \to \infty \tag{37}$$

and $\Delta z \to \Delta z_d$ such that $\bar{f}(\Delta z_d) = f_d$. Thus, the proof of convergence is completed. Further, all these convergences become exponential with order of $e^{-\alpha t}$ with some positive constant $\alpha > 0$. The details of the rigorous proof of exponential convergence is omitted in this paper due to the page limitation. Fortunately, we conclude that we do not need to assume the uniform boundedness of joint angles $|q_i(t) - q_i(0)|$ $(i = 1 \sim 5)$ in the proof of this exponential convergence.

IV. NUMERICAL SIMULATION

In this section, some results of numerical simulations are shown. The initial condition is given in Table I, and the desired state is shown in Table II. All the physical parameters of the thumb used in the simulations are given in Table III. Fig. 6 shows the 3-Dimensional graphics expressing simulation of "Blind Touching". In this figure, the initial pose and the final one are shown. The red circle area on the xy-plane is the contact area induced by deformation of the finger-tip. The blue line in the xy-plane is the trajectory of the center of contact area on the task plane. We see from this figure that by rolling the finger-tip of the thumb moves toward the desired position $\boldsymbol{x_d}$, the center of contact area $\boldsymbol{x_c}$ converges to the $\boldsymbol{x_d}$. Fig. 7 shows the transient responses of the rolling constraint forces λ_X, λ_Y and the touching force f. We see from this figure that both rolling constraint forces converge to zero. The settling time of λ_X is 0.4 [sec], and that of λ_Y is 0.6 [sec]. It means that the rolling movement is

TABLE I

INITIAL CONDITION OF THE THUMB ROBOT MODEL

Variable	Value
$\boldsymbol{q}$	$(0.0, 0.0, 0.69, 1.58, 0.61)^{\mathrm{T}}$ [rad]
$\boldsymbol{x_0}$	$(0.0, 0.06, 0.01)^{\mathrm{T}}$ [m]
$f(\Delta z)$	0.0 [N] $(\Delta z = 0$ [m])

TABLE II

DESIRED TOUCHING FORCE AND CONTACT POINT POSITION, AND DAMPING COEFFICIENT OF THE THUMB ROBOT MODEL

Parameter	Value
f_d	0.2 [N]
$\boldsymbol{x_d}$	$(0.005, 0.062, -\Delta z)^{\mathrm{T}}$ [m]
$\boldsymbol{C}$	$\mathrm{diag}(0.001, 0.0009, 0.0002, 0.0001, 0.00005)$

TABLE III

PHYSICAL PARAMETERS OF THE THUMB ROBOT MODEL

Physical parameter	Value
1st link length l_1	0.01 [m]
2nd link length l_2	0.05 [m]
3rd link length l_3	0.03 [m]
4th link length l_4	0.02 [m]
1st link mass center l_{g_1}	0.05 [m]
2nd link mass center l_{g_2}	0.025 [m]
3rd link mass center l_{g_3}	0.015 [m]
4th link mass center l_{g_4}	0.01 [m]
1st link mass m_1	0.02 [kg]
2nd link mass m_2	0.02 [kg]
3rd link mass m_3	0.015 [kg]
4th link mass m_4	0.01 [kg]
1st link inertia I_1	$\mathrm{diag}(0.17, 0.17, 0.25)\times 10^{-6}$ [kg·m^2]
2nd link inertia I_2	$\mathrm{diag}(4.17, 4.17, 0.25)\times 10^{-6}$ [kg·m^2]
3rd link inertia I_3	$\mathrm{diag}(1.13, 1.13, 0.19)\times 10^{-6}$ [kg·m^2]
4th link inertia I_4	$\mathrm{diag}(0.33, 0.33, 0.13)\times 10^{-6}$ [kg·m^2]
Radius of finger tip r	0.01 [m]
Stiffness coefficient k	2.0×10^5 [N/m^2]
Damping scalar function ξ	$8.0 \times 10^3 \times (2r\Delta z - \Delta z^2)\pi$

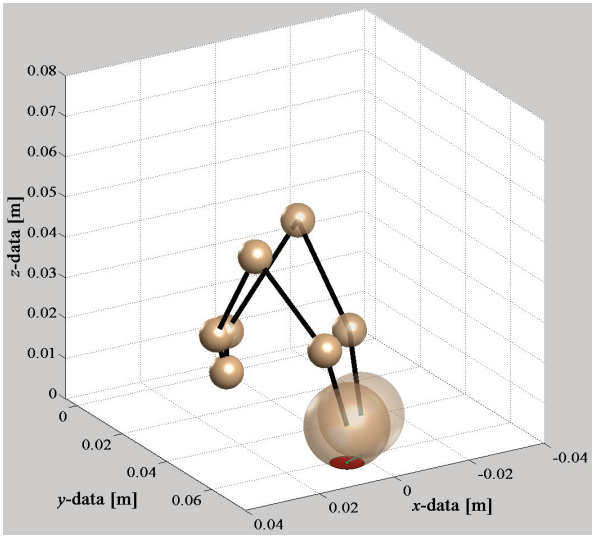

Fig. 6. 3-Dimensional graphics of the simulation of "Blind Touching"

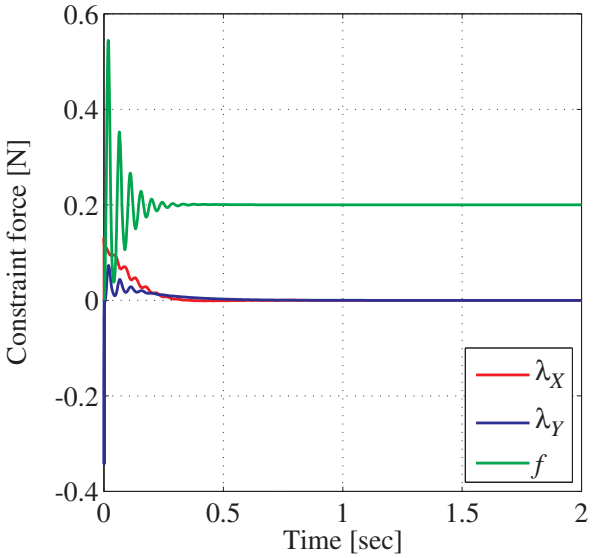

Fig. 7. Transient responses of rolling constraint forces λ_X, λ_Y and touching force f

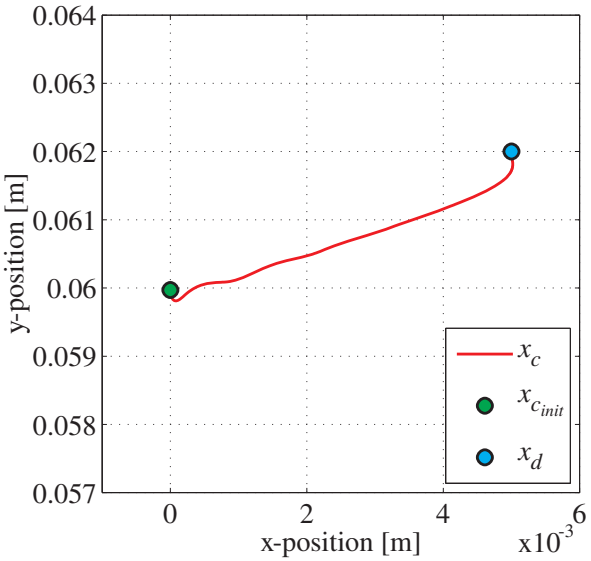

Fig. 9. Trajectory of position $\boldsymbol{x_c}$ of the center of contact area on the xy-plane

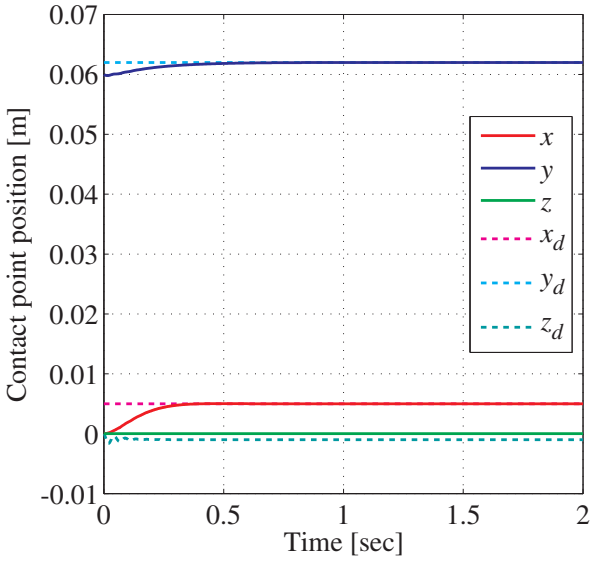

Fig. 8. Transient response of position $\boldsymbol{x_c}$ of the center of contact area

terminated at the $\boldsymbol{x_d}$. Also the touching force f converges to the desired force $f_d = 0.2$ [N] within 0.3 [sec]. Fig. 8 shows the transient response of position of the center of contact area $\boldsymbol{x_c}$. We see from this figure that x_c and y_c converge to the desired values x_d and y_d, respectively. The settling time of the x-component is 0.4 [sec], and that of the y-component is 0.6 [sec]. In contrast, z_c does not converge to $z_d = -\Delta z$ because this steady-state error generates the touching force f. To keep z_c at zero, the finger-tip should not be detached from the task space during movement. Fig. 9 shows the trajectory of position of the center of contact area $\boldsymbol{x_c}$ in the task plane. By rolling the finger-tip on the task plane, the center of contact area converges to the desired position.

Figs. 10∼12 show the simulation results when the desired position is given as one of the time-dependent value. The time-dependent desired contact point given here is shown in Table. IV. It is seen from Fig. 10 that even though the desired position is time-dependent, the touching force converges to the desired value quickly. Also the rolling constraint forces λ_X and λ_Y converge to zero. Figs. 11 and 12 show that the position of the center of contact area converges to the desired position, obviously.

V. CONCLUSION

This paper discussed possibility of "Blind Touching" by using a 5 D.O.F. thumb robot model. The results of numerical simulations suggest that "Blind Touching" proposed in this paper can be realized by using a sensory-motor coordinated signal that is constructed on the basis of the kinematic information of the thumb itself, and measured data of joint angles and angular velocities without using any external visual, force or tactile sensing.

In the future work, we shall consider the situation of non-contact phase between the finger-tip and the task plane, and then, consider a control strategy in order to cope with transition from the non-contact phase to the contact phase.

TABLE IV
TIME-DEPENDENT DESIRED CONTACT POINT $\boldsymbol{x_d}$

Time t [sec]	$\boldsymbol{x_d}$ [m]
$0.0 \sim 1.0$	$(0.002, 0.060, -\Delta z)^{\mathrm{T}}$
$1.0 \sim 2.0$	$(0.002, 0.062, -\Delta z)^{\mathrm{T}}$
$2.0 \sim 3.0$	$(-0.002, 0.062, -\Delta z)^{\mathrm{T}}$
$3.0 \sim 4.0$	$(-0.002, 0.058, -\Delta z)^{\mathrm{T}}$
$4.0 \sim 5.0$	$(0.002, 0.058, -\Delta z)^{\mathrm{T}}$
$5.0 \sim 6.0$	$(0.002, 0.060, -\Delta z)^{\mathrm{T}}$
$6.0 \sim 8.0$	$(0.0, 0.060, -\Delta z)^{\mathrm{T}}$

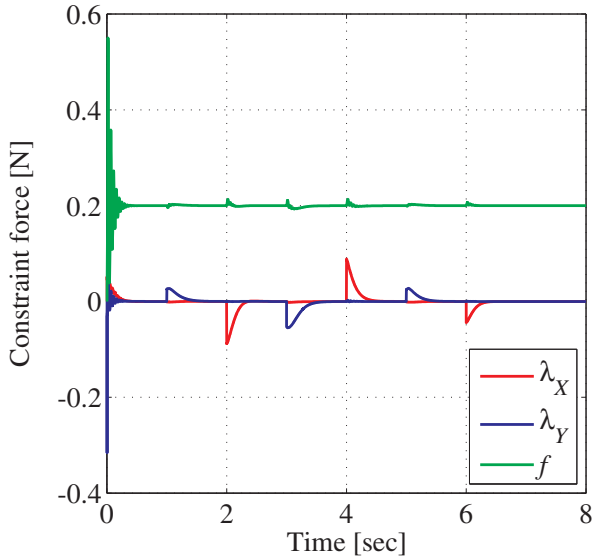

Fig. 10. Transient responses of rolling constraint forces λ_X, λ_Y and touching force f in the case of time-dependent desired contact position $\boldsymbol{x_d}$

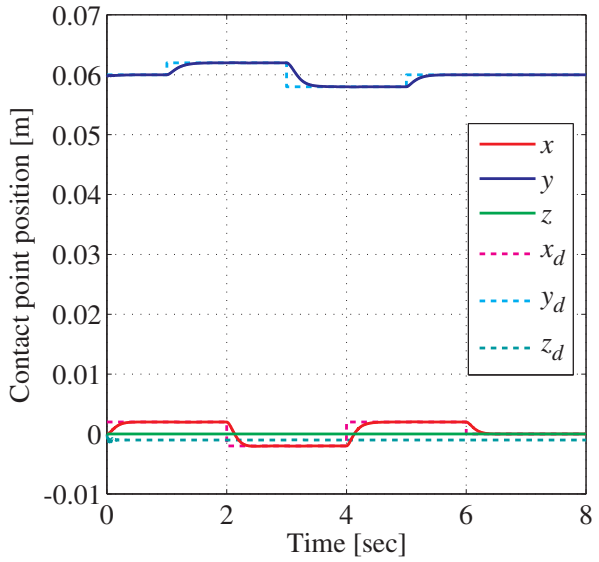

Fig. 11. Transient responses of position $\boldsymbol{x_c}$ of the center of contact area in the case of time-dependent desired contact position $\boldsymbol{x_d}$

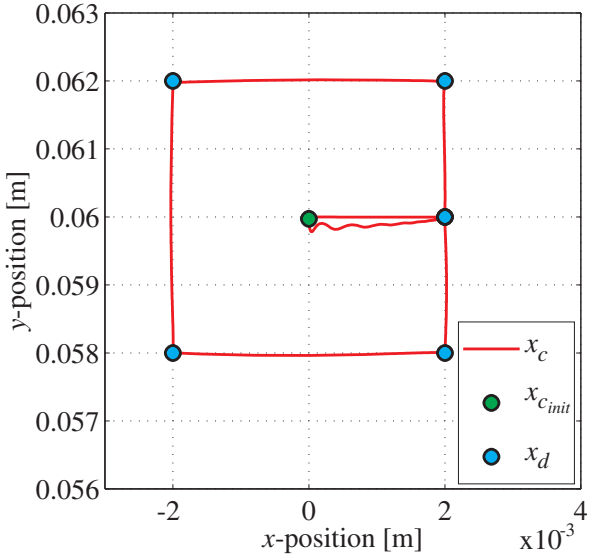

Fig. 12. Trajectory of position $\boldsymbol{x_c}$ of the center of contact area on the xy-plane in the case of time-dependent desired contact position $\boldsymbol{x_d}$

At present, we have already obtained interesting preliminary results on smooth transition from the non-contact phase to the contact one by regulating gains f_d and c_i of $\boldsymbol{C}$. The details will be presented at the conference. Also we will extend this approach to the arbitrary surfaces such as a cylinder, and so on. Further, applications to more practical situations should be discussed, that is, one of haptic devices to operate a cell phone, remote controller, hand-held music boxes, or human-machine interface like a game controller, and so on in place of the human thumb.

VI. ACKNOWLEDGMENTS

This work was partially supported by the Ministry of Education, Science, Sports and Culture, Grant-in-Aid for Young Scientists (B), 18760205, 2006.

REFERENCES

[1] J.R. Napier, *Hands,* Princeton Univ. Press, Princeton, NJ; 1993.
[2] M.R. Cutkovsky, *Grasping and Fine Manipulation*, Kluwer Academic, Dordrecht, Netherlands; 1985.
[3] R.M. Murray, Z. Li, and S.S. Sastry, *Mathematical Introduction to Robotic Manipulation*, CRC Press, Boca Raton; 1994.
[4] K.B. Shimoga, "Robot grasp synthesis algorithms: A survey," *Int. J. Robotics Research*, vol.15, no.3, 1996, pp.230-266.
[5] A.M. Okamura, N. Smaby, and M.R. Cutkovsky, "An overview of dexterous manipulation," *Proc. of IEEE Int. Conf. Robotics and Automation*, SanFrancisco, CA, 2000, pp.255-262.
[6] A. Bicchi, "Hands for dexterous manipulation and robust grasping: A difficult road towards simplicity," *IEEE Trans. Robotics and Automation*, vol.16, no.6, 2000, pp.652-662.
[7] L.Y. Chang and Y. Matsuoka, "A kinematic thumb model for the ACT hand," *Proc. of IEEE Int. Conf. Robotics and Automation*, Orlando, FL, 2006, pp.1000-1005.
[8] S. Arimoto, P.T.A. Nguyen, H.-Y. Han, and Z. Doulgeri, "Dynamics and control of a set of dual fingers with soft tips," *Robotica*, vol.18, no.1, 2000, pp.71-80.
[9] S. Arimoto, R. Ozawa, and M. Yoshida, "Two-dimensional stable blind grasping under the gravity effect," *Proc. of IEEE Int. Conf. Robotics and Automation*, Barcelona, Spain, 2005, pp.1208-1214.
[10] M. Yoshida, S. Arimoto, J.-H. Bae, "Stability analysis of 2-D object grasping by a pair of robot fingers with soft and hemispherical ends," *Proc. of 3rd IFAC Workshop on Lagrangian and Hamiltonian Methods for Nonlinear Control*, Nagoya, Japan, 2006, pp.257-262.
[11] S. Arimoto, M. Yoshida, and J.-H Bae, "Stability of 3-D object grasping under the gravity and nonholonomic constraints," *Proc. of Int. Symp. Mathematical Theory of Networks and Systems*, Kyoto, Japan, 2006, MoP07.5
[12] D.J. Montana, "The kinematics of contact and grasp," *Int. J. Robotics Research*, vol.7, no.3, 1988, pp.17-32.
[13] S. Arimoto, *Control Theory of Non-linear Mechanical Systems – A Passivity-based and Circuit-theoretic Approach*, Oxford University Press, NY; 1996.
[14] M. Takegaki and S. Arimoto, "A new feedback method for dynamic control of manipulators," *ASME J. Dynam. Syst., Measurement, Control*, vol. 102, 1981, pp. 119-125.